Effects of Finite Weight Resolution and Calibration Errors on the Performance of Adaptive Array Antennas

MATTIAS WENNSTRÖM, Student Member, IEEE
TOMMY ÖBERG
ANDERS RYDBERG, Member, IEEE
Uppsala University
Sweden

Adaptive antennas are now used to increase the spectral efficiency in mobile telecommunication systems. A model of the received carrier-to-interference plus noise ratio (CINR) in the adaptive antenna beamformer output is derived, assuming that the weighting units are implemented in hardware. The finite resolution of weights and calibration is shown to reduce the CINR. When hardware weights are used, the phase or amplitude step size in the weights can be so large that it affects the maximum achievable CINR. It is shown how these errors makes the interfering signals "leak" through the beamformer and we show how the output CINR is dependent on power of the input signals. The derived model is extended to include the limited dynamic range of the receivers, by using a simulation model. The theoretical and simulated results are compared with measurements on an adaptive array antenna testbed receiver, designed for the GSM-1800 system. The theoretical model was used to find the performance limiting part in the testbed as the 1 dB resolution in the weight magnitude. Furthermore, the derived models are used in illustrative examples and can be used for system designers to balance the phase and magnitude resolution and the calibration requirements of future adaptive array antennas.

Manuscript received October 29, 1999; revised August 21 and December 16, 2000; released for publication December 16, 2000.

IEEE Log No. T-AES/37/2/06329.

Refereeing of this contribution was handled by L. M. Kaplan.

This work was sponsored by the Swedish National Board for Industrial and Technical Development under Contract P9302916-6.

Authors' address: Uppsala University, Signaler and System, Box 528, SE-751, 20 Uppsala, Sweden.

I. INTRODUCTION

Using adaptive antennas at base stations (BS) in cellular systems has either shown to improve the capacity or to extend the radio coverage by increasing the carrier-to-interference ratio (CIR) at either the mobile station (MS) receiver or the BS receiver. The increased link CIR allows for a reduction in frequency reuse distance, thereby increasing the spectrum efficiency of the cellular system [1, 2].

The maximum achievable CIR in the BS receiver depends on the characteristics of the radio channel as well as the architecture of the receiver, defined as the hardware channel. One option for implementing the receiver is the hybrid-digital-analog beamformer (ABF), where the adaptive algorithm is implemented in software using a digital signal processor (DSP) and the beamformer weights are implemented in hardware [3]. Thus, the beamforming can be carried out on the RF or IF frequency, using digitally controlled analog phase-shifters and attenuators. The signals are split into a digital path and an analog path, as shown in Fig. 1. The benefits with the ABF is that it can be used as an add-on system on existing BS receivers, where the output from the ABF is connected to the ordinary BS receiver. Another implementation option is the fully digital beamformer (DBF) [4], where both the adaptive algorithm and the weighting of the signals is performed in DSP software. The DBF is flexible and allows for system upgrades by changing the DSP software, but requires a complete substitution of the BS equipment.

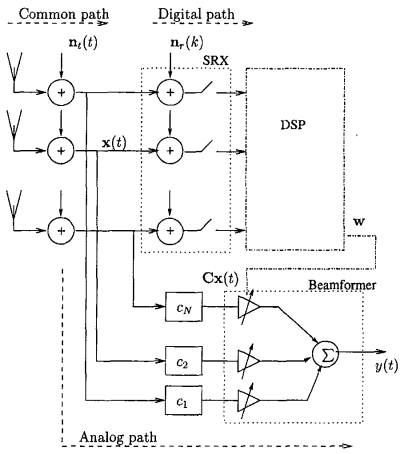

Fig. 1. Signal model of adaptive antenna.

The topic of this paper is to investigate how the hardware implementation of the weights and the following limited accuracy of the calibration of an ABF type of beamformer limits the performance of an adaptive array antenna. The aim is to develop a theoretical model of the hardware channel. The model can be used to balance the resolution in phase and

magnitude of the weighting units and to find the requirements on the calibration accuracy. Furthermore, the effects of finite word length in the DSP and the sampling receivers (SRX) that introduces quantization errors and limits the dynamic range of the receiver is discussed. Due to the nonlinear nature of dynamic range limiting, it is not included in the derived theoretical hardware channel model, hence the aim of the paper is only partly accomplished.

However, to extend the simplified model, both computer simulations and practical measurements using an adaptive antenna testbed was performed. These measures are used to validate the theoretical model and find in which ranges of operation the model is correct. The testbed, designed for use in a GSM-1800 system, is of ABF type and operates in receiving mode only. The simulation model includes the saturation effects from the limited dynamic range of the SRXs, to give a more accurate prediction of the adaptive antenna performance, especially at high input signal levels, where the SRXs are close to saturation.

Implementation errors on adaptive antenna arrays has previously been studied by several authors. The previous work can be separated into the following four categories.

A. Sampling Receivers

If the signal amplitude exceeds the maximum amplitude level of the analog-to-digital converter (ADC) in the SRX, nonlinear signal distortion will occur, and performance will quickly degrade. Also, the ADC introduces quantization noise which defines the lower limit of the SRX dynamic range. Previous studies by Hudson [5] and Takahashi, et al. [6] investigated the necessary number of ADC bits to achieve a certain level of interference suppression. Hudson studied the quantization of received signals and concluded that eight bits in the ADC was necessary to give 40 dB interference suppression with a ten element array. The number of ADC bits must be chosen to cover the whole dynamic range of the received signals, which can be substantial due to the near-far ratio and the fading in the radio channel.

B. Digital Signal Processor

The finite word length in the DSP affects the numerical stability and accuracy of matrix inversions used by some algorithms. Nitzberg studied the required word length to achieve desirable performance by using the optimal weights [7]. It was showed that the case with a single interference source requires the highest precision in the DSP (the largest DSP word length). Performance limiting errors in the DSP depends also on the choice of algorithm. For instance, many algorithms use the covariance matrix to estimate the beamformer weights. Due to the time-variant mobile channel the weights have to be updated frequently, and only the most recent samples are reliable for estimating the covariance matrix. The number of samples used in the estimation is an important parameter for the performance. Reed, Mallet, and Brennan studied this [8], and showed how the CIR on the adaptive antenna output depends on the number of used samples and the number of antennas (size of covariance matrix).

C. Weighting Units

The weighting units have finite accuracy determined by the type of weight used, and the number of control bits from the DSP. Analog weights can be implemented in various ways, as two phase-shifters in parallel, as two multipliers on the in-phase and quadrature branch, respectively, or as a phase-shifter and a multiplier in series connection [9]. The effect of quantization of weights have previously been studied in [10–12].

D. Calibration

A calibration must be performed to match the phase and amplitude of the different hardware channels. The calibration must also track variations in time due to temperature, humidity, etc and also be transparent and have no or a small noticeable effect on the normal operation of the adaptive array antenna [13]. Depending on the calibration method used, there will be a limited resolution in the calibration process and the residual calibration error will degrade the performance. Calibration errors was studied by Tsoulos, et al. [14–15], where measurements on an adaptive array using a calibration algorithm were presented. Wennström, et al. presented an on-line calibration algorithm that is transparent to main antenna operation, continuously tracking the changes in antenna channels [16]. The algorithm use a feedback of the output RF signal, and thus allows the use of, for example, the least mean square (LMS) algorithm for updating the corrected weights.

The derivations in this work do not depend on the actual implementation of the weighting units or the choice of the algorithm for calibrating the ABF. We assume a generic error model and the differences in weighting units enter through the variance of the weight errors and maximum value of the calibration error in phase and amplitude. The obtained results can be used to find the effects of different implementation techniques on the total performance of an adaptive antenna array of the ABF type in use in a mobile communication system. The performance bottlenecks are identified to help the designer to achieve a balanced dimensioning of the adaptive array antenna.

The paper is organized as follows. In Section II the hardware channel model is derived. Section III

describes the adaptive antenna testbed and Section IV describes the results from measurements and simulations. Conclusions are presented in Section V.

II. HARDWARE CHANNEL MODEL

In this section, the hardware channel model is derived. Fig. 1 shows the ABF with the analog weighting path and the digital path connected to the SRXs. It is assumed that all signals are represented by their complex baseband equivalents. The noise generated in the low noise amplifiers in the receiver front-end and the noise received by the N antennas are modeled as an equivalent $N \times 1$ noise vector, $\mathbf{n}_t(t)$, which is assumed to be spatially and temporally white.[1] We assume that $\mathbf{n}_t(t)$ is a vector with zero mean variables and covariance matrix $\mathbf{R}_{\mathbf{n}_t} = \sigma_t^2\mathbf{I}$.

To isolate the performance evaluation to the hardware channel, the simplest possible radio propagation channel is assumed; two narrowband signals impinge on a uniform linear array (ULA) antenna from two distinct azimuthal directions θ_d and θ_i.

The signal received by the N antennas can then be described by the $N \times 1$ vector $\mathbf{x}(t)$ as

$$\begin{aligned}\mathbf{x}(t) &= \mathbf{x}_d(t) + \mathbf{x}_i(t) + \mathbf{n}_t(t) \\ &= \mathbf{a}(\theta_d)s_d(t) + \mathbf{a}(\theta_i)s_i(t) + \mathbf{n}_t(t)\end{aligned} \quad (1)$$

where $\mathbf{a}(\theta_d)$ and $\mathbf{a}(\theta_i)$ is the complex valued array response vector in azimuth direction θ_d and θ_i, respectively, including antenna element gain and polarization. The baseband signals $s_d(t)$ and $s_i(t)$ denote the desired and interferer signal, respectively.

In the model, the SRXs are replaced by limiters and a noise source $\mathbf{n}_r(t)$. This noise represents the internal noise generated in the receivers and the quantization noise generated in the sampling process. The corresponding signal vector in the DSP can thus be written as

$$\mathbf{x}_{\mathrm{DSP}}(t_k) = \mathrm{sat}[\mathbf{a}(\theta_d)s_d(t_k) + \mathbf{a}(\theta_i)s_i(t_k) + \mathbf{n}(t_k)] \quad (2)$$

where t_k represents the sampling instants and $\mathbf{n}(t_k)$ is the sum of front-end thermal noise $\mathbf{n}_t(t)_{t=t_k}$, quantization noise and receiver noise $\mathbf{n}_r(t)_{t=t_k}$:

$$\mathbf{n}(t_k) = \mathbf{n}_t(t_k) + \mathbf{n}_r(t_k). \quad (3)$$

The saturation operator, sat[·], hard-limits the quadrature signals, above a certain amplitude level. The maximum amplitude level in each quadrature branch before saturation is dependent on the automatic gain control (AGC) setting of the receivers and the dynamic range of the ADC. If the signal voltage amplitude for any of the quadrature branches exceeds the maximal allowed amplitude, the signal is distorted. From here on, the nonlinear effects from signal saturation are not considered, to make the analysis analytically tractable.

B. Calibration

The aim of the calibration is to estimate the transfer function of the hardware channel between the SRX and the summation point after the weighting units. The estimated transfer functions for each hardware channel is used to compensate the corresponding weight in software before it is multiplied with the signal and summed in the beamformer. This compensation is important because the weights are calculated based on the signals from the SRX but applied to the signals entering the weighting units. We make the assumption that the channel between the SRX and the weighting units is wideband compared with the received narrowband signals and that the transfer function is flat over the passband of interest. This implies that the transfer function can be represented by a complex number representing the gain/attenuation and the phase shift of the channel. Note that this assumption might not be valid in a wideband system as W-CDMA, if the transfer function cannot be assumed to be flat over the whole system bandwidth.

By introducing the complex matrix $\mathbf{C} = \mathrm{diag}(c_1,\ldots,c_N)$, the relation of the signal at the weighting units $\mathbf{x}_w(t)$ and the SRX $\mathbf{x}(t)$ can be expressed as

$$\mathbf{x}_w(t) = \mathbf{C}\mathbf{x}(t). \quad (4)$$

The off-diagonal elements in $\mathbf{C}$, which here are assumed negligible,[2] represent the mutual coupling between the channels in the beamformer. Assume that the algorithm calculates the weight vector $\mathbf{w}_{\mathrm{DSP}}$, based on the received signals $\mathbf{x}_{\mathrm{DSP}}(t_k)$. To compensate for the differences in the receiving channels, the weights are preadjusted to

$$\mathbf{w} = (\mathbf{C}^{-1})^{\mathrm{H}}\mathbf{w}_{\mathrm{DSP}} \quad (5)$$

where $(\cdot)^{\mathrm{H}}$ denotes hermitian transpose. The analog beamformer output signal $y(t)$ will then be

$$y(t) = \mathbf{w}^{\mathrm{H}}\mathbf{x}_w(t) = \mathbf{w}_{\mathrm{DSP}}^{\mathrm{H}}\mathbf{C}^{-1}\mathbf{C}\mathbf{x}(t) = \mathbf{w}_{\mathrm{DSP}}^{\mathrm{H}}\mathbf{x}(t). \quad (6)$$

Thus the effect of the transfer function $\mathbf{C}$ is canceled.

When the calibration is performed, the weights are adjusted to measure the transfer function for different weight settings. This implies that the accuracy in the weight settings will also have an impact on the

[1] This assumption means that we assume that no other interference sources are present which have a directional property. Furthermore, the white noise generated in each antenna branch in the front end are assumed mutually independent. Thus the noise is both temporally and spatially white.

[2] The coupling between two hardware channels is extremely small and the main contribution to the mutual coupling comes from the antenna array elements. This coupling is neglected to simplify the derivation.

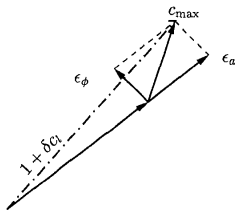

Fig. 2. Squared calibration error bounded by $c_{\max}^2 = \epsilon_a^2 + \epsilon_\phi^2$.

accuracy of the calibration. Hence, the calibration has a finite accuracy, so $\mathbf{C}$ will not be known exactly. Also, due to temperature drift, humidity variations and component aging, the calibration correction matrix has a time variant residual error and will not describe the actual transfer function. Assume that the array has been calibrated by some arbitrary method and let the matrix $\hat{\mathbf{C}}$ be the calibration correction matrix that is stored in the DSP. If the calibration is error free, then $\hat{\mathbf{C}} = \mathbf{C}$. We can now write $\hat{\mathbf{C}}^{-1}\mathbf{C} = \mathbf{I} + \delta\mathbf{C}$, where $\delta\mathbf{C}$ is a diagonal matrix with complex elements, representing the relative calibration errors. Writing the diagonal elements of $\delta\mathbf{C}$ as $\delta c_l = d_l e^{j\phi_l}$, we separate the relative calibration errors into a magnitude error d_l and a phase error ϕ_l. The magnitude d_l is assumed to be bounded in the range $[\pm\epsilon_a]$ and the phase error ϕ_l is in the range $[\pm\epsilon_\phi]$. As the phase and magnitude errors are orthogonal, see Fig. 2, the maximum calibration error squared, $c_{\max}^2$ is given as

$$c_{\max}^2 = \epsilon_a^2 + \epsilon_\phi^2. \tag{7}$$

B. Output Signal Power

As a performance measure for the adaptive antenna, we use the carrier-to-interference plus noise ratio (CINR) of the beamformer output signal. An expression for the output power is derived and the different terms are identified as desired (carrier) terms and interferer and noise terms to be used to calculate the CINR. Some simplifying assumptions are made to make the analysis possible. The saturating effect of the SRX (2), is not taken into consideration, and the sources of the two signals, $s_d(t)$ and $s_i(t)$, are assumed to be sufficiently separated in azimuth to make the spatial correlation close to zero. Due to the finite step size in the hardware weighting units, the weights $\mathbf{w}$ will be quantized and an error vector $\delta_{\mathbf{w}}$ is introduced. The total weight error covariance matrix is $\sigma_w^2\mathbf{I}$, where an example of how σ_w^2 can be derived for a specific type of weighting units is presented in Section IIIC. The signal on the beamformer output can be written as

$$\begin{aligned} y(t) &= (\mathbf{w} + \delta_{\mathbf{w}})^{\mathrm{H}}\hat{\mathbf{C}}^{-1}\mathbf{C}\mathbf{x}(t) = (\mathbf{w} + \delta_{\mathbf{w}})^{\mathrm{H}}(\mathbf{I} + \delta\mathbf{C})\mathbf{x}(t) \\ &= \mathbf{w}^{\mathrm{H}}\mathbf{x}(t) + \text{error terms} \end{aligned} \tag{8}$$

and the power of the beamformer output signal is then written as

$$E\{|y(t)|^2\} = E\{((\mathbf{w} + \delta_{\mathbf{w}})^{\mathrm{H}}\hat{\mathbf{C}}^{-1}\mathbf{C}\mathbf{x}(t))((\mathbf{w} + \delta_{\mathbf{w}})^{\mathrm{H}}\hat{\mathbf{C}}^{-1}\mathbf{C}\mathbf{x}(t))^{\mathrm{H}}\}. \tag{9}$$

Using (8) and assuming that the elements of the stochastic vectors $\delta_{\mathbf{w}}$, $\mathbf{x}(t)$ and the matrix $\delta\mathbf{C}$ are mutually uncorrelated, (9) is simplified to

$$\begin{aligned} E\{|y(t)|^2\} &= \mathbf{w}^{\mathrm{H}}E\{\mathbf{x}(t)\mathbf{x}^{\mathrm{H}}(t)\}\mathbf{w} + E\{\delta_{\mathbf{w}}^{\mathrm{H}}\mathbf{x}(t)\mathbf{x}^{\mathrm{H}}(t)\delta_{\mathbf{w}}\} \\ &\quad + \mathbf{w}^{H}E\{\delta\mathbf{C}\mathbf{x}(t)\mathbf{x}^{\mathrm{H}}(t)\delta\mathbf{C}^{\mathrm{H}}\}\mathbf{w} \\ &\quad + E\{\delta_{\mathbf{w}}^{\mathrm{H}}\delta\mathbf{C}\mathbf{x}(t)\mathbf{x}^{\mathrm{H}}(t)\delta\mathbf{C}^{\mathrm{H}}\delta_{\mathbf{w}}\}. \end{aligned} \tag{10}$$

If the SRXs are saturated, the weight errors $\delta_{\mathbf{w}}$ will become mutually correlated and the independence assumption between the weight errors $\delta_{\mathbf{w}}$ and the signal $\mathbf{x}(t)$ is not valid. Note that $\mathbf{x}(t)$ is the analog RF signal (1) which is not saturated.

The terms in (10) can be identified as the ideal output term, the weight error term, the calibration error term, and the combined weight-calibration error term, respectively. The combined weight-calibration error term contains the product of the two error variables and is neglected in the following. The weight and calibration error term are quadratic forms with the error terms $\delta_{\mathbf{w}}$ and $\delta\mathbf{C}$ and are assumed to be sources of interference. This is a pessimistic assumption, because these terms also include some signal which are correlated with the desired signal and might add to the output carrier power.

1) *Ideal Output Term*: The first term in (10) is the output signal from a beamformer without calibration or weight quantization errors. This term is dominant in the DBF type of antenna, where weighting of the signals is performed in the DSP itself, so weight errors are negligible and calibration errors of the type considered here is not present.

The performance of the error-free beamformer is dependent on the algorithm used for calculating the weights $\mathbf{w}$. In a temporal reference algorithm or a direction-finding algorithm the number of samples m used in the estimation of the covariance matrix compared with the number of antennas is an important factor [8]. Due to the finite length of the training sequence, the temporal correlation between the two signal sources $s_d(t)$ and $s_i(t)$ will be non-zero. Also the azimuthal separation angle between the two sources, quantified as the spatial correlation, will have impact on the performance of the algorithms.

For the analog signal $\mathbf{x}(t)$ the following holds

$$\begin{aligned} \mathbf{R}_{xx} &= E\{\mathbf{x}(t)\mathbf{x}^{\mathrm{H}}(t)\} \\ &= \sigma_d^2\mathbf{a}(\theta_d)\mathbf{a}^{\mathrm{H}}(\theta_d) + \sigma_i^2\mathbf{a}(\theta_i)\mathbf{a}^{\mathrm{H}}(\theta_i) + \sigma_t^2\mathbf{I} \\ &= \mathbf{R}_d + \mathbf{R}_i + \sigma_t^2\mathbf{I}. \end{aligned} \tag{11}$$

where $\mathbf{R}_d$ and $\mathbf{R}_i$ are the desired and interfering signal covariance matrix, respectively. Also, σ_d^2 and σ_i^2 is the

desired and interfering signal power, respectively. The ideal term in (10) can now be written as

$$\begin{aligned}\mathbf{w}^{\mathrm{H}}E\{\mathbf{x}(t)\mathbf{x}^{\mathrm{H}}(t)\}\mathbf{w} &= \mathbf{w}^{\mathrm{H}}\mathbf{R}_d\mathbf{w} + \mathbf{w}^{\mathrm{H}}\mathbf{R}_i\mathbf{w} + \sigma_t^2|\mathbf{w}|^2 \\ &\leq \mathbf{w}^{\mathrm{H}}\mathbf{R}_d\mathbf{w} + \mathbf{w}^{\mathrm{H}}\mathbf{R}_i\mathbf{w} + N\sigma_t^2 w_{\max}^2\end{aligned} \tag{12}$$

where $w_{\max}$ is the maximum allowed weight magnitude, determined by the hardware and σ_t^2 is the thermal noise variance. The first term in (12) represents the power in the desired, or useful signal. The second term is the interference output power, which also is dependent on the beamformer weights $\mathbf{w}$. Clearly, the adaptive beamformer tries to calculate the weight $\mathbf{w}$ so that the quadratic form $\mathbf{w}^{\mathrm{H}}\mathbf{R}_i\mathbf{w}$ is small, to suppress the interferer. This term will be non-zero if the algorithm has not converged, which can be the case for recursive algorithms in a time-variant radio channel or for block algorithms if a finite number of samples are used in the weight estimation. Note that the weight error $\delta_{\mathbf{w}}$ is due to the use of hardware weighting units, and will be present even if the exact, interference cancellation weight $\mathbf{w}$ has been estimated. To mitigate this residual error, a feedback of the beamformer output signal $y(t)$ could be used to iteratively tune the weights so the weight and calibration errors decreases. A method for this was presented in [16].

The third term in (12) represents the sum of noise power from N uncorrelated noise sources with same power $w_{\max}^2\sigma_t^2$.

2) *Weight-Error Term*: The second term in (10) is due to weight quantization and is expanded as

$$\begin{aligned}&E_{x,\delta_{\mathbf{w}}}\{\delta_{\mathbf{w}}^{\mathrm{H}}\mathbf{x}(t)\mathbf{x}^{\mathrm{H}}(t)\delta_{\mathbf{w}}\} \\ &\quad= E_{x,\delta_{\mathbf{w}}}\{\mathrm{Tr}\{\mathbf{x}(t)\mathbf{x}^{\mathrm{H}}(t)\delta_{\mathbf{w}}\delta_{\mathbf{w}}^{\mathrm{H}}\}\} \\ &\quad= \mathrm{Tr}\{E_x\{\mathbf{x}(t)\mathbf{x}^{\mathrm{H}}(t)\}E_{\delta_{\mathbf{w}}}\{\delta_{\mathbf{w}}\delta_{\mathbf{w}}^{\mathrm{H}}\}\} \\ &\quad= \sigma_w^2\mathrm{Tr}\{\mathbf{R}_{xx}\} \\ &\quad= \sigma_w^2(\sigma_d^2|\mathbf{a}(\theta_d)|^2 + \sigma_i^2|\mathbf{a}(\theta_i)|^2 + N\sigma_t^2).\end{aligned} \tag{13}$$

The property that the trace of the covariance matrix is equal to the sum of the received signal power and that the signal and the weight errors are mutually independent was used. Note that this only is valid under the assumption of nonsaturated SRXs. The weight errors $\delta_{\mathbf{w}}$ cause signal power to leak through the beamformer, with a power proportional to the total impinging power. The amount of "leaking" power is determined by weight error variance σ_w^2.

3) *Calibration-Error Term*: The third term in (10) includes the diagonal matrix $\delta\mathbf{C}$ that models the calibration errors. The structure is a Hermitian form and we find the upper bound as

$$\begin{aligned}\mathbf{w}^{\mathrm{H}}E_{\mathbf{x}}\{\delta\mathbf{C}\mathbf{x}(t)\mathbf{x}^{\mathrm{H}}(t)\delta\mathbf{C}^{\mathrm{H}}\}\mathbf{w} &= \mathbf{w}^{\mathrm{H}}\delta\mathbf{C}\mathbf{R}_{xx}\delta\mathbf{C}^{\mathrm{H}}\mathbf{w} \\ &\leq \lambda_{\max}|\mathbf{w}^{\mathrm{H}}\delta\mathbf{C}|^2 \\ &\leq \mathrm{Tr}\{\mathbf{R}_{xx}\}|\mathbf{w}^{\mathrm{H}}\delta\mathbf{C}|^2\end{aligned} \tag{14}$$

where $\lambda_{\max}$ is the largest eigenvalue of the Hermitian matrix $\mathbf{R}_{xx}$. The bound cannot be tighter, since the bound is attained when the error vector $\mathbf{w}^{\mathrm{H}}\delta\mathbf{C}$ is colinear with the eigenvector to $\mathbf{R}_{xx}$ associated with the largest eigenvalue. The largest eigenvalue has to be found on a case-by-case basis. Thus, we resort to examine the worst possible case. Since $\mathbf{R}_{xx}$ is Hermitian positive definite, all eigenvalues are real and positive and the largest eigenvalue is always less or equal to the trace of $\mathbf{R}_{xx}$.

Furthermore, the vector norm expression cannot be evaluated, because it depends on the magnitude of the weights and the calibration errors. An upper bound can be found by assuming that all weight magnitudes are smaller than $w_{\max}$, which is the maximum possible weight that can be steered out by the hardware weighting units. Similarly, the upper bound of the calibration errors $c_{\max}$ is defined. Thus by setting $|w_l|^2 = w_{\max}^2$ for all weights and $|c_l|^2 = c_{\max}^2$ for all calibration paths, we can write the vector norm in expression (14) as

$$\begin{aligned}|\mathbf{w}^{\mathrm{H}}\delta\mathbf{C}|^2 &= |w_1^*c_1|^2 + \cdots + |w_N^*c_N|^2 \\ &\leq |w_1|^2|c_1|^2 + \cdots + |w_N|^2|c_N|^2 \\ &\leq N w_{\max}^2 c_{\max}^2\end{aligned} \tag{15}$$

where the Cauchy–Schwartz inequality was used. Now, use that the trace of $\mathbf{R}_{xx}$ is equal to the total impinging power on the array and rewrite (14) as

$$\begin{aligned}&\mathbf{w}^{\mathrm{H}}E_x\{\delta\mathbf{C}\mathbf{x}(t)\mathbf{x}^{\mathrm{H}}(t)\delta\mathbf{C}^{\mathrm{H}}\}\mathbf{w} \\ &\quad\leq N w_{\max}^2 c_{\max}^2(\sigma_d^2|\mathbf{a}(\theta_d)|^2 + \sigma_i^2|\mathbf{a}(\theta_i)|^2 + N\sigma_t^2).\end{aligned} \tag{16}$$

Similar to the weight error term (13), the total impinging power, described by the trace of $\mathbf{R}_{xx}$ is weighted by a proportionality constant. The constant in this case depends on the maximum calibration error $c_{\max}$ and is bounded by the squared root of the sum of the squared magnitude and phase errors (7).

4) *Output CINR*: Using the equations above, we now derive an expression for the beamformer output CINR. The power of the desired, or useful signal in the beamformer output is described by the first term in (12). The two other terms in (12), and (13) and (16) are assumed to be interferer and noise power terms. Thus, the beamformer output CINR can be expressed as

$$\begin{aligned}\mathrm{CINR} \geq (\mathbf{w}^{\mathrm{H}}\mathbf{R}_d\mathbf{w})/(\mathbf{w}^{\mathrm{H}}\mathbf{R}_i\mathbf{w} + N\sigma_t^2 w_{\max}^2 + (\sigma_w^2 + N c_{\max}^2 w_{\max}^2) \\ (\sigma_d^2|\mathbf{a}(\theta_d)|^2 + \sigma_i^2|\mathbf{a}(\theta_i)|^2 + N\sigma_t^2)).\end{aligned} \tag{17}$$

To maximize this expression, the weight calculation algorithm should make $\mathbf{w}^H\mathbf{R}_i\mathbf{w}$ as small as possible. Thus the weight vector $\mathbf{w}$ will yield an antenna radiation pattern with "nulls" in the direction of the interfering sources.

The expression (17) was derived using several simplifications, but it illustrates how the desired and interfering signal power "leaks" through the beamformer, due to calibration errors and weight quantization. The system designer should choose the implementation of the weighting units so that the weight error variance σ_w^2 is equal in magnitude to the term $Nc_{\max}^2 w_{\max}^2$ that represents the calibration errors. In the limit when calibration errors and the weight quantization errors approaches zero, i.e. $c_{\max} \to 0$ and $\sigma_w^2 \to 0$, the CINR approaches the well-known expression for CINR of a DBF,

$$\mathrm{CINR}_{\mathrm{DBF}} \simeq \frac{\mathbf{w}^H\mathbf{R}_d\mathbf{w}}{\mathbf{w}^H\mathbf{R}_i\mathbf{w} + N\sigma_t^2 w_{\max}^2}. \tag{18}$$

How the different terms in the denominator dominate in different cases is investigated by the simulations and the measurements presented in Section IV.

III. ADAPTIVE ANTENNA TESTBED

To validate the theoretical expression for the CINR, measurements on an adaptive antenna testbed was made. The hardware and the used sample matrix inversion (SMI) algorithm are described in this section. The weight error variance for the testbed specific type of weighting units is derived, followed by a discussion of the measurement setup. The testbed was developed to follow the GSM-1800 standard, however, the standard is not used to its full extent. No control or signalling channels for call setup is implemented and during the measurements, only the traffic channel (TCH) in the GSM-1800 standard were used. Call setup was performed manually during an initialization phase and synchronization of sampling instants were handled by manually tuning the SRX. Furthermore, 8 bit ADCs were used, which gives an unsufficient dynamic range to comprise the fading variations and near-far ratio of an actual GSM channel.

A. Hardware

In this section the adaptive antenna testbed is described briefly. For a more detailed description of the testbed, refer to [17]. The testbed has ten antenna elements that can be mounted in linear, circular or any arbitrary array configuration. Double-down conversion from 1.721 GHz is performed with a variable LO at 1.62 GHz and second step with a fixed LO at 71 MHz. The receivers have a measured noise figure of 11 dB, a maximal voltage gain of 75 dB, and an input IP3 point at +2 dBm. The ADC use 8 bits and 270 kHz sampling rate per quadrature channel to digitize the signals and the data is transferred to the DSP using a 32 bit parallel bus. The isolation between the quadrature channels was measured to 75 dB. The DSP calculates the weights using the software running on three TMS320C40 signal processors out of seven on-board TMS320C40.

The testbed has two independent sets of weights with ten weighting units per set. Each digitally controlled weighting units consists of two 180° phase-shifters and a 50 dB logarithmic attenuator connected in series. The reason for choosing logarithmic attenuators, is that in the design process, it was believed that a high dynamic range of the weights was beneficial. The logarithmic attenuator was thus chosen in favor of the linear one. The logarithmic attenuator has a range of attenuation of 50 dB but it was later discovered that a 50 dB range is overabundant. The beamformer seldom uses weight magnitudes below −15 dB. The weighting units have a calculated noise figure of 6 dB and a measured third order intercept point of +6 dBm. The temperature drift was measured to 0.1 dB and 1° per weighting unit and hour of operation. Hence, frequent recalibration or on-line calibration is necessary to maintain the highest level of performance.

Calibration of the antenna array is performed prior to normal operation of the testbed. A CW signal is injected at one antenna element at a time by directional couplers. The received signal is compared with the beamformer output signal and the phase and magnitude of the transfer functions $c_l e^{j\phi_l}$ can be calculated. The calibration has an accuracy of 1° in phase and 0.75 dB in magnitude [17]. Using (7), the relative calibration error constant $c_{\max}^2$ can be calculated as $c_{\max}^2 = 8.4 \cdot 10^{-3}$.

B. SMI Algorithm

The DSP calculates the weights by using the SMI algorithm [18]. As a reference signal, the 26 bit training sequence in the midamble of a GSM-1800 timeslot is used. The covariance matrix of the received signals and the cross-correlation between the received signal vector $\mathbf{x}(t_k)$ and the reference signal $s_d(t_k)$ is estimated using $m = 26$ samples. The signal covariance matrix estimate is then

$$\hat{\mathbf{R}}_{xx} = \frac{1}{m}\sum_{k=1}^{m} \mathbf{x}_{\mathrm{DSP}}(t_k)\mathbf{x}_{\mathrm{DSP}}^H(t_k). \tag{19}$$

The cross-correlation is estimated as

$$\hat{\mathbf{r}}_{xd} = \frac{1}{m}\sum_{k=1}^{m} \mathbf{x}_{\mathrm{DSP}}(t_k)s_d^H(t_k) \tag{20}$$

where $(\cdot)^H$ denotes the complex conjugate transpose. Thus, the reference signal $s_d(t_k)$ is a modulated,

prerecorded copy of the training sequence of the desired signal, stored in the DSP memory.

The SMI weight vector is now calculated as

$$\mathbf{w} = \gamma \hat{\mathbf{R}}_{xx}^{-1} \hat{\mathbf{r}}_{xd} \tag{21}$$

where the factor γ scales the weights for full utilization of the dynamic range of the hardware weights. The weight vector is adjusted by the calibration matrix $\hat{\mathbf{C}}$ and applied to the RF signals $\mathbf{x}_w(t)$, see Fig. 1.

The SMI algorithm has a fast convergence rate as compared with other known algorithms, e.g. the LMS algorithm. The SMI algorithm, approximately $2N$ samples in the block are required to obtain weights that give a CINR within 3 dB of the optimum achievable CINR [8]. Here, $N = 8$ antennas where used, so $m > 2N$.

C. Weight Error Variance

Given the phase and magnitude resolution of these hardware parts, we derive the weight error variance. Weight error variances for other weight implementations can be found in [9], especially for the linear amplitude weighting technique.

An arbitrary weight with magnitude M and phase θ with magnitude accuracy $\pm\epsilon_M$ and phase accuracy $\pm\epsilon_\theta$ can be written as

$$w = Me^{j\theta}. \tag{22}$$

Assuming that the magnitude and phase errors are small, and by differentiation of both sides of (22) and collecting terms gives

$$|dw|^2 = dM^2 + M^2 d\theta^2 \tag{23}$$

where dM is the magnitude error and $d\theta$ is the phase error. We assume that dM and $d\theta$ are independent, random variables and that dM is uniformly distributed in the interval $\pm\epsilon_M$ and $d\theta$ uniformly distributed in the interval $\pm\epsilon_\theta$. Taking the expectation value of (23) then gives

$$\sigma_w^2 = \sigma_M^2 + M^2\sigma_\theta^2 \tag{24}$$

where $\sigma_M^2 = \epsilon_M^2/3$ and $\sigma_\theta^2 = \epsilon_\theta^2/3$.

The total error variance (24) is dependent on the weight magnitude M. An upper bound on the weight error variance is given by replacing M with the maximum weight magnitude $w_{\max}$, thus

$$\sigma_w^2 \le \sigma_M^2 + w_{\max}^2\sigma_\theta^2 = \tfrac{1}{3}(\epsilon_M^2 + w_{\max}^2\epsilon_\theta^2). \tag{25}$$

The contribution from the phase error to the sum in (25) is thus dependent on the maximal weight magnitude. Note for large attenuator settings, say -15 dB, the difference to the next weight setting of -16 dB is very small on a linear scale. Hence small values of the weight amplitudes make the weight quantization noise small. The largest error variance occurs when the weight amplitude is set at its maximum value.

The weighting units has a phase resolution of 1° and uses logarithmic attenuators with 1 dB magnitude step size and a 50 dB range between $[-2\text{ dB}, -52\text{ dB}]$. Thus, the constant $w_{\max} = -2$ dB. The weight magnitude variance is then calculated using (25) as

$$\begin{aligned}
\sigma_M^2 &= \frac{(0.5\cdot(10^{1/20}-1))^2}{3} = 1.24\cdot 10^{-3} \\
\sigma_\theta^2 &= \frac{\left(\frac{0.5\cdot\pi}{180}\right)^2}{3} = 0.025\cdot 10^{-3} \\
w_{\max}^2 &= 10^{-2/10} \\
\Rightarrow \sigma_w^2 &\le 1.25\cdot 10^{-3}
\end{aligned} \tag{26}$$

where a conversion from dB scale to the linear scale is performed. This implies that the proportionality constant $Nc_{\max}^2 w_{\max}^2$ in (17) is an order of magnitude larger than the weight error constant σ_w^2. Thus, the calibration errors limit the performance for the testbed, which is verified by the simulations. It should also be noted that the main contribution to the weight error variance of the testbed arises from magnitude errors (the step attenuators). The phase error contribution is two orders of magnitude smaller than the magnitude error contribution. Noticeable is that the weight magnitude variance is calculated for the worst case using logarithmic weighting units, i.e., at minimum attenuation. When the weight magnitude is smaller the steps are smaller, due to the logarithmic nature of the weights. A simple calculation yields that at a weight magnitude of -16 dB, the phase error variance and the magnitude error variance are equal.

D. Measurement Setup

Measurements were performed in a laboratory, to validate the performance of the adaptive array antenna in an easy controllable signal environment. The front-end array antenna is replaced by an 8×8 Butler matrix. The output ports of the Butler matrix are connected to the receivers. The eight input ports are used to emulate signals impinging on a ULA from eight different directions. The use of a Butler matrix will ideally make the array response vectors orthogonal, i.e., $\mathbf{a}^H(\theta_i)\mathbf{a}(\theta_d) = 0$ and thus, the spatial correlation between the two signals is zero. But the hardware Butler matrix have imperfections from the manufacturing, in our case a peak error 0.8 dB in amplitude and 8.5° in phase. These errors will make the array response vectors $\mathbf{a}(\theta_d)$ and $\mathbf{a}(\theta_i)$ nonorthogonal which corresponds to a more realistic signal environment.

Two signal generators were connected to the Butler matrix to emulate signals impinging ideally from

$-61°$ and $-7.2°$. The signal generators transmitted pseudorandom binary (PRBS) data as traffic data. In GSM-1800, eight different training sequences (bit patterns) are defined, and we used number 0 and number 4 in the GSM-1800 standard for the two signal sources, respectively. The training sequence is then used in the SMI algorithm to calculate the beamformer weights.

E. Comparison of Measurements and Theory

In practice, the CINR in (17) cannot be measured, due to the inability to separate the desired signal from the interfering and noise signal. Instead, we measured a modified CIR on the adaptive antenna output, denoted $\mathrm{CIR}_{\mathrm{out}}$, in fact, we measured the carrier-plus-noise to interferer-plus-noise ratio, where "noise" includes the thermal noise, calibration error noise, and the weight quantization noise.

To perform measurements, the levels of the two signals were set and the adaption of the beamformer weights was started. To measure $\mathrm{CIR}_{\mathrm{out}}$ for an arbitrary weight realization, the adaption was stopped at an arbitrary time instant. When the adaption was stopped, the weight update also stopped and the CIR in the beamformer output could be measured. This was made in a two step procedure where the interferer power and the desired signal power was measured separately. The signal generator emulating the desired signal was turned off and the ABF interferer plus noise output power was measured using a spectrum analyzer. Then the desired signal's generator was turned on and the interfering signal's generator was turned off and the ABF desired signal-plus-noise output power was measured. By assuming that the system is linear and the superposition principle holds, the $\mathrm{CIR}_{\mathrm{out}}$ can be expressed by the use of equation (9)–(16) as

$$\mathrm{CIR}_{\mathrm{out}} \leq \frac{\mathbf{w}^{\mathrm{H}}\mathbf{R}_d\mathbf{w} + N\sigma_t^2 w_{\max}^2 + (\sigma_w^2 + Nc_{\max}^2 w_{\max}^2)(\sigma_d^2|\mathbf{a}(\theta_d)|^2 + N\sigma_t^2)}{\mathbf{w}^{\mathrm{H}}\mathbf{R}_i\mathbf{w} + N\sigma_t^2 w_{\max}^2 + (\sigma_w^2 + Nc_{\max}^2 w_{\max}^2)(\sigma_i^2|\mathbf{a}(\theta_i)|^2 + N\sigma_t^2)}. \tag{27}$$

The second and third term in the numerator of (27) makes the $\mathrm{CIR}_{\mathrm{out}}$ estimate too optimistic. Therefore the expression (27) is larger or equal to the actual $\mathrm{CIR}_{\mathrm{out}}$. The term $\mathbf{w}^{\mathrm{H}}\mathbf{R}_i\mathbf{w}$ is the interferer signal power that leaks through the correct beamformer weights, and is usually very small, if the DOA separation is large enough, which is the case in our measurements. It will therefore be neglected in the following. The term $\mathbf{w}^{\mathrm{H}}\mathbf{R}_d\mathbf{w}$ expresses the received power from the desired signal. If the DOA separation is large enough it can be approximated as a constant K multiplied with the desired signal power σ_d^2, where K is the array gain, including amplifiers in the front end and in the weighting units, degraded by the spatial and temporal correlation of the two signals. By making these simplifications, (27) can be rewritten as

$$\mathrm{CIR}_{\mathrm{out}} \lesssim \frac{K\sigma_d^2 + N\sigma_t^2 w_{\max}^2 + (\sigma_w^2 + Nc_{\max}^2 w_{\max}^2)(\sigma_d^2|\mathbf{a}(\theta_d)|^2 + N\sigma_t^2)}{N\sigma_t^2 w_{\max}^2 + (\sigma_w^2 + Nc_{\max}^2 w_{\max}^2)(\sigma_i^2|\mathbf{a}(\theta_i)|^2 + N\sigma_t^2)}. \tag{28}$$

Clearly, if the desired signal power σ_d^2 is large compared with the interfering signal power σ_i^2 and noise power σ_t^2, then the $\mathrm{CIR}_{\mathrm{out}}$ in (28) will differ from the $\mathrm{CINR}_{\mathrm{out}}$, due to the large term in the numerator. If the interferer-to-carrier ratio is high, say 20 dB, then (28) will resemble (17) well. Conclusive, we expect the theory and the measurements to correspond well for high interference-to-noise power ratios.

IV. SIMULATION AND MEASUREMENT RESULTS

A. Simulation Setup

The simulation was performed to imitate the testbed as much as possible. The simulation model is shown in Fig. 1. Two Gaussian minimum shift keying (GMSK) modulated signals were generated with 8 samples per symbol. The Gaussian filter had an impulse response length of 6 symbols and the normalized bandwidth was 0.3. As training sequences, the training sequences 0 and 4 given by the GSM-1800 standard were used. The received signal was quantized and the calculated weights were used with finite accuracy. Two impinging signals from the same directions as generated by the Butler matrix in the measurements were used in the simulations. Furthermore, calibration errors were also introduced, to emulate the testbed.

The ADCs used the sampling frequency of 270 kHz, the same as in the adaptive antenna testbed. The covariance matrix (19) and the cross-correlation vector (20) were estimated using the 26 complex samples. The direction of arrivals (DOAs) for the two signals were equal to the DOAs in the measurements, described in Section III. The array response vectors were slightly distorted to emulate the 0.8 dB magnitude errors and 8.5° phase errors in the Butler matrix and to make the spatial correlation non-zero.

The weight vector was calculated and normalized using (21) and the calculated weight vector was quantized to the desired accuracy in magnitude and phase and applied to the signals at the weighting units after multiplication with the matrix $(\mathbf{C}^{-1})^{\mathrm{H}}$ as described by (5).

B. Validation of Simulation Model

After adaption, the same procedure to measure $\mathrm{CIR}_{\mathrm{out}}$ as described in Section IIIE for the

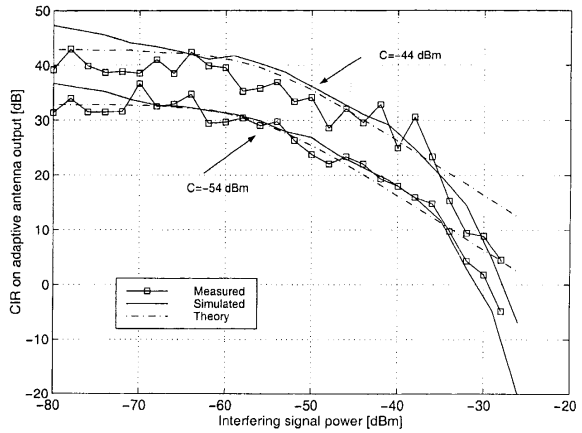

Fig. 3. CIR_{out} as function of interferer power. Comparisons between measurements, simulation and theory (equation (28)). Carrier power constant at −44 dBm and −54 dBm, respectively. Noise level at −76 dBm.

measurements was used to measure the CIR_{out} in the simulation, to make the comparisons fair. A GMSK modulated PRBS signal using $m_l = 200$ samples was used to estimate the CIR_{out}. To verify the theoretical model and the simulation results, a comparison is made in Fig. 3. The simulation parameters are set equal to the parameters used in the adaptive antenna testbed, e.g., 8 bit ADCs and 1° and 1 dB weight accuracy. Fig. 3 shows the measured output CIR, denoted CIR_{out} as a function of interfering signal power, when the desired signal power was held constant at two different levels, −44 dBm and −54 dBm, respectively. The figure also shows the corresponding simulation results and the theory, described by (28). The measured curves constitute mean values over ten measurements and the simulated are averaged over 100 simulations. The standard deviation is 7 dB and 0.8 dB in measurements and simulations respectively. The theoretical expression does not consider the limited dynamic range of the ADC, so the theoretical CIR_{out} is larger than the measured and simulated CIR_{out} when the interfering signal saturates the ADC.

The theory, equation (28), predicts the CIR_{out} to reach a constant level when the interferer is decreased below the thermal noise level, i.e., when the dominating term in the denominator of (28) is the noise term $N\sigma_t^2 w_{max}^2$. This is verified by the measurements and the level is determined by the desired signal power and the weight and quantization error variances. The simulated curve does not fit into this level at the low interference situation. An attempt to explain this is that the noise level was not correctly set in the simulations, so the noise term $N\sigma_t^2 w_{max}^2$ does not dominate over the interference power σ_i^2 even for the lowest interference power.

Noticeable is however the agreement of theory and measurements for high carrier-to-noise ratios (CNRs). It was in this region were the CIR_{out} approximation, equation (28), was less accurate.

C. Number of ADC Bits

By increasing the number of bits used in the ADC, the dynamic range of the SRX is increased, as shown in the simulation results of Fig. 4. Here the same calibration errors and weight errors as in the testbed is used. With a larger dynamic range, the SRX can receive a signal with higher power without saturating. Increasing the number of bits from 10 to 12 will not improve the output CIR in this scenario, because the SRX is not saturated for these input levels. The limiting factor in the 10 and 12 bit case is the weight and calibration errors.

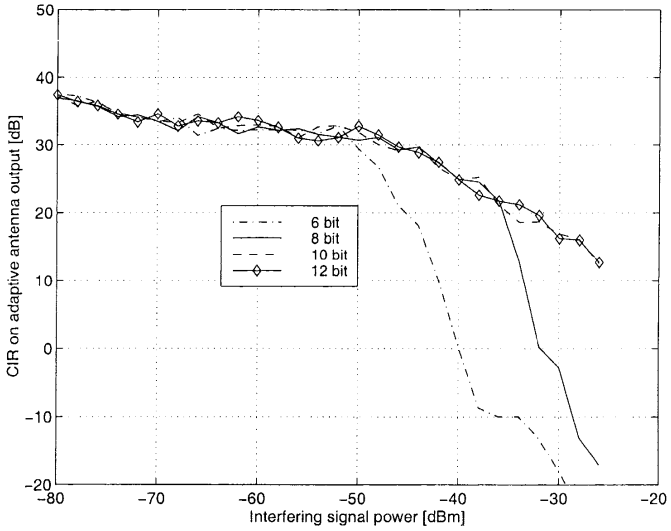

Fig. 4. Simulated CIR_{out} [dB] when number of ADC bits is varied as function of CIR. Carrier constant at CNR = 42 dB and interferer power varied. Note that abscissa shown in interferer-to-carrier ratio.

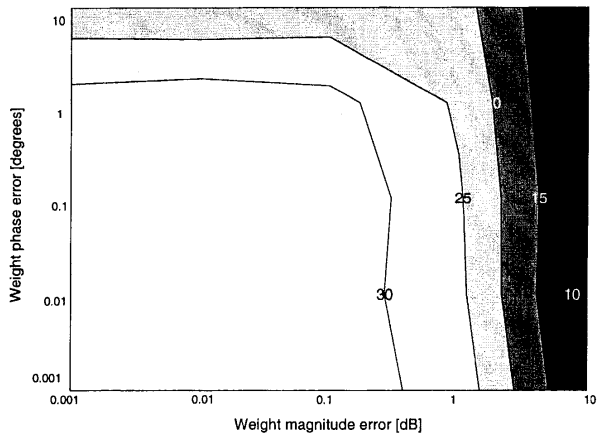

Fig. 5. Simulated CIR_{out} [dB] as function of quantization of phase and magnitude of weights, $CIR_{in} = -15$ dB, CNR = 42 dB. Shades refer to different CIR_{out} levels with white and black being largest and smallest, respectively.

D. Weight Accuracy

To solely investigate the impact of weight accuracy on the performance of the adaptive antenna array, we assumed a perfect calibration, i.e., $\hat{\mathbf{C}}^{-1}\mathbf{C} = \mathbf{I}$. Also, an 8 bit ADC was used to make comparisons with the adaptive antenna testbed possible. The CIR_{out} was measured for different settings of the range of the relative weight errors ϵ_M and ϵ_θ.

The CIR_{in} that a single virtual omnidirectional antenna would measure was set to -15 dB and the CNR was 42 dB. The CIR_{out} on the adaptive antenna output was estimated and the results are presented in Fig. 5.

Fig. 5 shows that a 30 dB CIR_{out} can be achieved if the phase and magnitude quantization steps are less than 1° and 0.3 dB. Thus, the maximal CIR improvement in this scenario is 45 dB and decreasing the weight quantization steps further will not improve the antenna performance for this particular DOA and signal levels. To achieve a larger improvement, more antennas can be used, which will make the spatial correlation smaller and the ability to suppress interferers larger.

E. Calibration Errors

We investigate how the calibration accuracy affects the CIR_{out} in Fig. 6. This figure displays CIR_{out} as a function of the weight error variance, for four different calibration accuracies. A weight error variance less than 10^{-5} will not further improve the CIR because the calibration errors limit the maximum achievable CIR.[3] To compare with the testbed, with a weight variance of $1.25 \cdot 10^{-3}$ the maximum achievable CIR_{out} in Fig. 6 is approximately 24 dB if the calibration is performed without errors. This should be compared to the measured 18 dB from the testbed in the same conditions. Thus, to improve the testbed performance, effort should be put to improve the calibration algorithm, in favor for improving the weight accuracy. Improving weight accuracy will raise CIR_{out} only a few dB.

When the weight errors are negligible, an amplitude calibration error of 1% gives a CIR_{out} degradation of 7–8 dB from the ideal case, with no errors. This is a severe degradation and the conclusion is that the calibration must have a high accuracy and also be performed frequently to maintain the adaptive antenna's interferer suppression performance over a long time of operation.

[3]This weight error variance could for example be achieved with 1° phase step size and 0.1 dB weight amplitude step size.

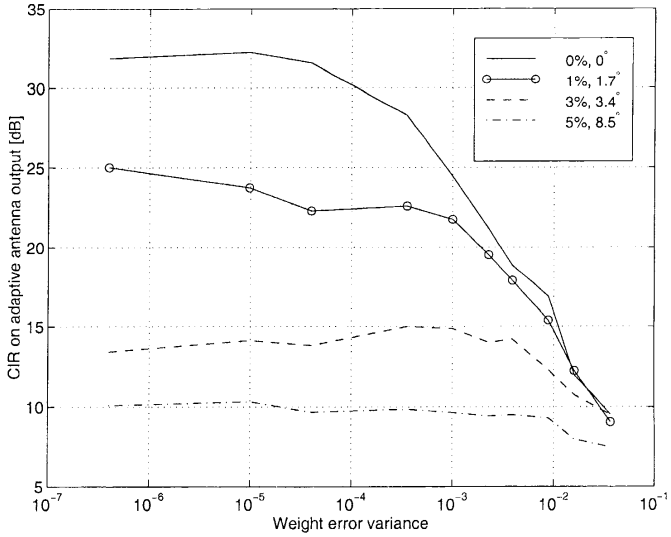

Fig. 6. CIR_{out} as function of weight quantization error for different calibration errors, $CIR_{in} = -15$ dB, CNR = 42 dB.

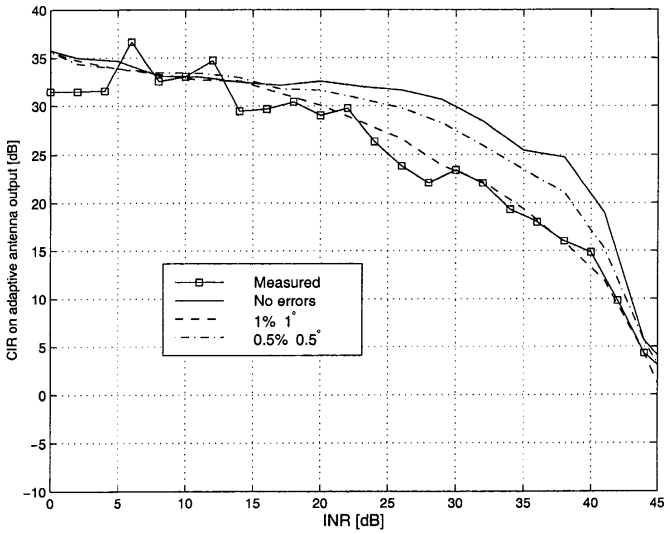

Fig. 7. CIR_{out} as function of INR for different calibration errors. CNR = 22 dB.

The effect of calibration errors when the CIR_{in} is varied by varying the interference-to-noise ratio (INR) is presented in Fig. 7. The CNR was held constant at 22 dB. A comparison with the adaptive antenna testbed was made, and the CIR_{out} was measured for different calibration errors and different CIR_{in}. The weight quantization steps were set to 1 dB and 1°. The measured curve fits the curve with calibration error of 1% in relative magnitude and 1° in phase. Furthermore, when INR < 22 dB, i.e., when CIR > 0 dB, the calibration errors have a negligible effect on the antenna performance. When the interferer power gets large, the output noise, described in (13) and (14), is increasing and the CIR decreases. When the total input power saturates the ADC, the CIR decreases abruptly and the antenna cannot maintain a CIR above 0 dB on the output. Note that the RF analog signal on the output from the adaptive antenna is not saturated. But the signal used in the DSP to calculate the weights is saturated and the CIR_{out} drops.

V. CONCLUSIONS

To study the performance degradation when implementing an adaptive antenna array algorithm in hardware, using an ABF type of beamformer, an expression for the output CINR was derived. Due to the complexity of the problem, involving nonlinear saturation effects, the derivation was only partly accomplished and some simplifications were made. The study showed how the weight quantization errors and calibration errors increase the output noise power, thus decreasing the output CINR. An important observation is that the decrease in CINR is proportional to the total impinging power on the array.

The theoretical results were verified and extended using an ABF type adaptive antenna testbed with ten array elements, working in the receive mode and designed to partly follow the GSM-1800 standard. To extend the testbed to support the GSM-1800 standard, protocol issues and random access channels must be handled for call set-up and handover situations [19]. Also, synchronization of sampling instants must be automatically handled; an algorithm for this is described in [20]. The fact that the GSM-1800 standard is not fully implemented does not affect the results here as long as the received signals are within the dynamic range of the ADCs, which for the testbed is not sufficiently large to comprise an actual GSM-1800 radio channel with fading variations and the near-far ratio. The weight resolution and calibration accuracy have an impact on the interference suppression capability of the adaptive antenna which affects the link budget only. Hence, the conclusions in this paper can be applicable to an ABF BS antenna and especially a GSM-1800 standard system with the reservation of the number of ADC bits.

The theoretical expressions were also verified using a simulation model of the hardware channel and allowed for an extension of the analytical model. The balance between weight accuracy and calibration accuracy showed that with a certain calibration accuracy, the output CINR could not improve above a certain limit, regardless of weight accuracy. Thus, the system designer should balance these two sources of error. For the testbed, it can be concluded that improving the calibration accuracy would gain more in output CIR as compared with improving the weight accuracy, the magnitude steps in the weighting units (1 dB) were too coarse, as compared with the phase accuracy (1°). Thus the bottleneck in the testbed is identified as the coarse magnitude steps. The system designer should put effort into making the phase and

magnitude error variances equal to minimize a large overhead in either the phase-shifter or attenuator accuracy. Note that it was assumed that the number of bits in the ADCs is sufficiently large, i.e., chosen so that the dynamic range is not a limitation of the system performance.

The extension of these results to other wireless standards depends on the complexity of the receivers. Using the ABF in a W-CDMA system is not feasible, even if the beamforming is carried out prior to the code correlator as in the multidimensional RAKE receiver [21]. Usually the channel model (1) is too simple to model a CDMA channel, although Naguib, Paulraj, and Kailath used it in one of their early derivations of the capacity improvement in using antenna arrays in CDMA systems [22]. In the multidimensional RAKE receiver, a set of weighting units for each RAKE finger and each user is required and the number of weighting units becomes very large, which is unpractical if they are implemented in hardware. Also, using a spread spectrum standard, the system bandwidth is increased and the transfer function of the hardware channel, defined as the matrix $\mathbf{C}$, could become a function of frequency. This makes the calibration more difficult, and the complexity of the compensation algorithm increases.

Conclusively, the results in the paper applies to systems where ABF is possible to implement, such as in the demonstrated narrowband GSM-1800 system and in systems where the spatial beamforming and the temporal equalization are separated. The results from the theoretical model affects the link budget only, in terms of the received CINR at the BS, as long as the received signals are within the dynamic range of the receivers. The results are also independent of the choice of weight calculation algorithm and calibration algorithm.

ACKNOWLEDGMENTS

The authors wish to acknowledge O. Gladh, L. Rexberg, and E. Sandberg at Ericsson Radio Access AB for financial and technical support. B. V. Andersson and M. Appelgren at Communicator are acknowledged for consultations regarding the measurements. The authors also acknowledge H. Andersson and M. Landing for the development of the adaptive antenna demonstrator and J. Strandell for measurement support.

REFERENCES

[1] Ho, M. J., Stuber, G. L., and Austin, M. D. (1998)
Performance of switched-beam smart antennas for cellular radio systems.
IEEE Transactions on Vehicular Technology, **47** (1998), 10–19.

[2] Swales, S. S., Beach, M. A., Edwards, D. J., and McGeehan, J. P. (1990)
The performance enhancement of multibeam adaptive base-station antennas for cellular land mobile radio systems.
IEEE Transactions on Vehicular Technology, **39** (1990), 56–67.

[3] Wennstrom, M. (1999)
Smart antenna implementation issues for wireless comunications.
Technical
report, Signals and Systems, Uppsala University, Sweden, 1999, Technical Licentiate Thesis in Signal Processing. (http://www.signal.uu.se/Publications/abstracts/l991.html).

[4] Litva, J., and Lo, T. (1996)
Digital Beamforming in Wireless Communications.
Boston: Artech House, 1996.

[5] Hudson, J. (1977)
The effects of signal and weight coefficient quantisation in adaptive array processors.
In *Proceedings of the NATO Advanced Study Institute of Signal Processing*, Reidel, Dordrecht, Netherlands, 1977, 423–428.

[6] Karasawa, Y., Takahashi, T., and Chiba, I. (1994)
The required resolution of A/D for null beamforming in a DBF antenna.
In *IEEE International Symposium Digest Antennas and Propagation*, New York, 1994, 128–131.

[7] Nitzberg, R. (1980)
Computational precision requirements for optimal weights in adaptive processing.
IEEE Transactions on Aerospace and Electronic Systems, **AES-16** (1980), 418–425.

[8] Reed, I. S., Mallet, J. D., and Brennan, L. E. (1974)
Rapid convergence rate in adaptive arrays.
IEEE Transactions on Antennas and Propagation, **AP-10**, 6 (1974), 853–863.

[9] Davis, R., and Sher, P. (1984)
Quantisation noise in adaptive weighting networks.
IEEE Transactions on Aerospace and Electronic Systems, **AES-20** (1984), 547–559.

[10] Nitzberg, R. (1976)
Effect of errors in adaptive weights.
IEEE Transactions on Aerospace and Electronic Systems, **AES-12** (1976), 369–373.

[11] Godara, L. (1985)
The effect of phase-shifter errors on the performance of an adaptive antenna-array beamformer.
IEEE Journal of Oceanic Engineering, **10** (1985), 278–284.

[12] Shatskii Voloshina, G. (1995)
The discretization effect of phase control on the noise-to-signal ratio in adaptive arrays.
Radioelectronics and Communication Systems, **38** (1995), 44–45; translated from *Izvestiya Vysshikh Uchebnykh Zavedenii Radioelektronika*, **38**, 7 (1995), 67–69.

[13] Beach, M., Brown, P., Dowds, M., Fonollosa, J., Greenaway, D., Kenington, P., Mayrargue, S., Monot, J. J., Passmann, C., Simmonds, C., Thibault, J., and Villino, G. (1998)
Requirements for flexible multi-standard adaptive antenna basestations.
Technical report AC347/FTC/A2.1/DS/P/002/b1, SUNBEAM Project, 1998.

[14] McGeehan, J., Tsoulos, G., and Beach, M. (1998)
Space division multiple acess (SDMA) field trials. Part 2: Calibration and linearity issues.
IEE Proceedings—Radar, Sonar and Navigation, **145** (1998), 79–84.

[15] Tsoulos, G., and Beach, M. (1997)
Calibration and linearity issues for an adaptive antenna system.
In *Proceedings of Vehicular Technology Conference*, Phoenix, AZ, 1997, 1597–1600.

[16] Wennström, M., Strandell, J., Öberg, T., Lindskog, E., and Rydberg, A. (2000)
Auto-calibrating adaptive array for mobile telecommunications.
IEEE Transactions on Aerospace and Electronic Systems, **36**, 2 (2000), 729–736.

[17] Landing, M., and Andersson, H. (1997)
Adaptive antenna for mobile telephone systems.
Technical report, Signals and Systems, Uppsala University, Sweden, 1997, Technical Licentiate Thesis in Electronics.

[18] Monzingo, R., and Miller, T. (1980)
Introduction to Adaptive Arrays.
New York: Wiley, 1980.

[19] Hagerman, B., and Andersson, S. (1999)
Adaptive antennas in wireless systems-basic background and field-trial results.
In *RVK99*, Karlskrona, Sweden, 1999.

[20] Lindskog, E. (1995)
Making SMI-beamforming insensitive to the sampling timing for GSM signals.
In *Proceedings of the Sixth International Symposium on Personal, Indoor and Mobile Radio Communications*, Toronto, Canada, 1995, 664–668.

[21] Dell'Anna, M., and Aghvami, A. H. (1999)
Performance of optimum and suboptimum combining at the antenna array of a W-CDMA system.
IEEE Journal on Selected Areas in Communications, **17** (1999), 2123–2137.

[22] Paulraj, A., Naguib, A. F., and Kailath, T. (1994)
Capacity improvement with base-station antenn arrays in cellular CDMA.
IEEE Transactions on Vehicular Technology, **43** (1994), 691–698.

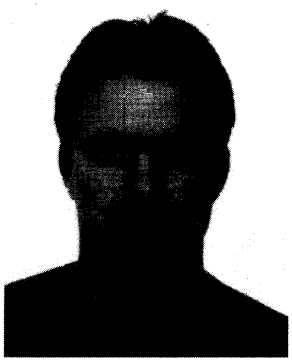

Mattias Wennström (SM'96) was born in 1972 in Uppsala, Sweden. He received the M.Sc. degree in engineering physics from Uppsala University in 1997.

Since March 1997, he has been a Ph.D. student in signal processing at the Signal and Systems Group at Uppsala University. He received his Licentiate degree in signal processing in 1999.

His main research interests are array antennas for wireless communications, effects on nonlinearities on wireless system performance and space time coding for channel capacity enhancements.

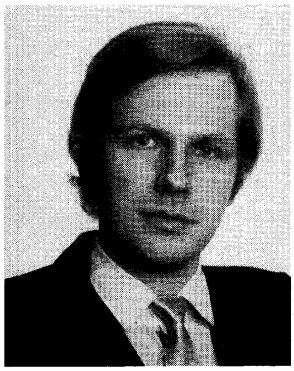

Tommy Öberg was born in Sundsvall, Sweden in 1950. He received a B.S. degree in physics and mathematics in 1976 and a Ph.D. degree in electrical engineering from Uppsala University, Institute of Technology, in 1982.

He joined Ericsson Radio Systems AB where he worked with radar systems and was responsible for investigations considering radar countermeasures, signal processing and antennas. From 1985 to 1987 he worked at Radiosystem Sweden AB with the GSM digital mobile telephone system. His responsibilities included investigations concerning the signal processing of this system to create a basis for new products. After that he was with Communicator Sensonik (former AB Teleplan) as a senior consultant in the field of radio and radar systems, and also part time at Uppsala University where he worked with research and teaching. Since October 1989 he has been with the University as Associated Professor (högskolelektor). He is responsible for courses in digital signal processing and communications. He is also responsible for several research projects and alsoinvolved as tutor (supervisor). His professional interests are mainly signal processing in telecommunication.

Dr. Öberg is the author of the textbook *Modulation, detektion och kodning* which will soon be published in English under the name *Modulation, detection and coding*.

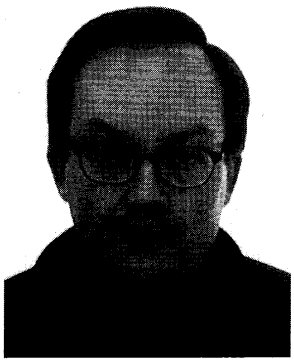

Anders Rydberg (M'89) was born in Lund, Sweden, in 1952. He received the M.Sc. degree from Lund Institute of Technology in 1976. He received the degree of Licentiate of Engineering and the Ph.D. degree, respectively, from Chalmers University of Technology, Sweden, in 1986 and 1988, respectively.

Between 1977 and 1983, he worked with development and research at the National Defense Research Establishment, ELLEMTEL Development Company, and the Onsala Space Observatory. From 1990 to 1991, he worked as a senior research engineer at Farran Technology Ltd., Ireland. In 1991, he was appointed Docent (Associated Professor) in Applied Electron Physics at Chalmers University of Technology. In 1992, he became an Associate Professor at the Signal and Systems Group, Uppsala University School of Technology. Since 1996, he is also Associate Professor and Research Leader part-time at the University College of Gavle-Sandviken, Sweden. His main interests are micro- and millimeter-wave solid state components and circuits for radio communication.

Dr. Rydberg has authored or co-authored more than 70 papers and is also a co-owner of one patent on applications of single-barrier-varactor diodes. He is a member of the editorial board for *IEEE Transactions on Microwave Theory and Techniques* and a delegate in the Swedish URSI-sections B and D.